Simplified Colloidal Method to Produce Nanostructured Au-Ag Films with Superconductivity in the Ambient

Subham Kumar Saha[1#], Rekha Mahadevu[1#], Pritha Mondal[1], Anand Sharma[1], Navyashree Vasudeva[1], and Anshu Pandey[1*]

[#]Equal Contribution

[1]Solid State and Structural Chemistry Unit, Indian Institute of Science, Bangalore 560012, India

*Correspondence to: anshup@iisc.ac.in

Abstract

Au-Ag nanostructures have been posited as potential room temperature, ambient pressure superconductors in past studies. Here we describe highly simplified methods that cause controlled precipitation of gold and silver colloids to produce nanostructured Au-Ag films that have been shown previously to exhibit unconventional electron transport phenomena and optical behaviour at under ambient or roughly ambient pressure and temperature conditions. The final material produced is comprised of a distribution of silver nanoparticles embedded into gold. The optical properties associated with these structures and films as well as their oxygen sensitivity are further discussed. The emphasis of this article is to enable researchers to synthesize these materials readily in their own laboratories and determine their properties.

Introduction

Gold and silver have been associated with metallic transport at a wide range of temperatures[1]. Recently, Thapa et. al.[2] showed the occurrence of resistive and magnetic transitions in Au-Ag nanostructures. The transition to a low resistance, diamagnetic state could be tuned, and the state itself was shown to exist at temperatures well above room temperature at ambient pressures. The methods described in the original report did not present a comprehensive survey of the preparative aspects of these materials. Further, key difficulties as well as qualitative characteristics of the process intermediates were not described. Here we present a detailed discussion of wet chemical methods that may be employed to prepare nanostructured Au-Ag films that have been posited to be ambient superconductors. We firstly describe the process involved in preparation of silver clusters. Methods to embed these into gold matrices are then discussed. The resultant materials comprise of a distribution of Ag particles in an Au matrix. Optical properties that are extremely useful in diagnosing reaction outcomes are described. The effect of air exposure on these materials is described.

Electrical properties of the silver-gold bimetallic system have generated significant scientific interest [2-9]. In our own investigations, we have observed emergent electrical, magnetic and optical properties in Au-Ag nanostructures that comprise of ~1 nm Ag clusters embedded into an Au matrix that distinguish these materials from other Au, Ag structures. The process of embedding Ag nanoparticles into an Au matrix is somewhat challenging due to several chemical and structural factors. Most notably, Ag and Au are soluble in each other at all concentrations and further have near identical lattice constants. These factors effectively eliminate the possibility of using strain to build these materials. We therefore found it most convenient to build these materials in two steps; namely to firstly prepare silver nanoparticles and subsequently to embed these into gold. An obvious problem is the dissimilar diffusivities of silver nanoparticles and species such as Au^0 or Au^{3+}. Here we approach this problem through a co-precipitation of silver and gold particles that are

eventually deposited on a substrate to prepare a film. The process is described in Figure 1. Broadly, this process bears similarities to the methods previously reported by us to prepare binary semiconductor nanocrystal assemblies[10, 11]. A key distinction between the metal-metal and the semiconductor-semiconductor system is however that while charge transfer alone can drive the formation of binary semiconductor assemblies, the formation of Au-Ag nanostructures requires actively destabilizing the Au, Ag colloid.

Silver nanoparticles are prepared by reducing solutions of silver nitrate in cetyltrimethylammonium bromide (CTAB) through sodium borohydride. In a typical reaction, $AgNO_3$ was added to aqueous solution of 10 ml of 0.1 M CTAB containing 1 ml of 1 M NH4Br, 40 µl of 0.1 M KI and 0.1 ml of 0.1 M NaOH. The reaction mixture is maintained at 50°C at this stage. During the course of our studies, we found that mildly basic conditions (~pH 8) improve reaction reliability. Further, a batch-to-batch variance in CTAB pH was noted which is ameliorated by the addition of NaOH. Over the period of 2 min the reaction mixture becomes turbid in part due to formation of silver halide precipitate. The precise time taken varies slightly with CTAB batch even when temperatures are maintained constant. With the reagent batches mentioned in the method section, we found that addition of sodium borohydride 90 s after $AgNO_3$ addition led to the best results. This corresponds to the addition of $NaBH_4$ ~10 s before turbidity appears. The optical spectrum immediately prior to $NaBH_4$ addition as well as the appearance of the dispersion are shown in Figure 2a and Figure 2a, inset.

The above process leads to nanoparticles with a diameter of approximately ~1 nm. Figure 2b shows the size distribution of a typical ensemble of Ag nanoparticles produced via this route. These results have been inferred using atomic force microscopy of silver nanoparticles deposited onto a mica substrate. For a typical measurement, the growth solution of the as-formed nanoparticles was drop-cast onto a mica substrate. This was allowed to stand for 5 minutes under a light source (~100 mW/cm^2 at sample). The growth solution was then removed by tilting the substrate and the residue left on the substrate was rinsed with deionized 18 M-Ohm water. As evident from Figure 1, with the scheme adopted, we obtain Ag nanoparticles with a median diameter of 1 nm and a range (0.25 to 3.25 nm). Optical spectra of these Ag nanoparticles are shown in Figure 2c. Further, the appearance of a typical solution is also shown (Figure 2c, photograph). As shown here, Ag nanoparticles produced through this scheme lack a well-defined silver Localized Surface Plasmon Resonance (LSPR) at ~3.1 eV [12-14]. The suppression of plasmons in small Ag particles is rather well known[15] and is usually explained by invoking electron-surface scattering processes for smaller particles at-least from the bulk perspective. We note that other effects, including a change in electronic density of states due to confinement may also operate on these sizes of Ag particles[16-18].

Immediately after the formation of Ag particles, we caused the formation of Au nanoparticles within the solution by the rapid introduction of aqueous 1 mM $HAuCl_4$. This is reduced by the residual sodium borohydride that persists in the reaction mixture after the previous step. This rapid reduction leads to the emergence of a distinctive brown coloration (Figure 2d, photograph) to the initially yellowish solution of silver nanoparticles. Figure 2d shows the typical spectra observed during the growth of Au nanoparticles. As evident, increased addition of $HAuCl_4$ at this stage leads to a more red-shifted Au absorbance feature. Continued $HAuCl_4$ addition leads to the eventual formation of large Au nanostructures with plasmon features at ~2.5 eV. However, for our purposes, we found it most convenient to restrict the $HAuCl_4$ addition to the point where the Au extinction feature is still located at 2.6 eV. A typical optical extinction spectrum is shown in Figure 2d (See also Figure 2d inset for a photograph of a typical sample at this stage of processing). We usually limit ourselves to this particular level of gold growth based on our observations of the behaviour of films prepared from these materials. Briefly, for larger amounts of gold growth, transitions to lower resistivity states become more erratic and difficult to achieve, consistent with increasingly filamentary transport in films. For smaller amounts of gold growth, films become largely metallic with evidence of silver rich regions. Regulation of Au to Ag ratio essentially leads to a change in the volume density of Ag nanoparticles within the final films. Based on our present understanding of this preparative method, controlling the Ag nanoparticle loading volume density does not allow control over the temperature at which the vanishing resistance state becomes accessible. However, it does affect the reliability with which such a state may be accessed.

As shown elsewhere[7] Au-Ag nanostructures containing a large number of Ag nanoparticles exhibit suppression of the usual Au and Ag Mie resonances. Instead, the optical spectra of these materials exhibit a broad non-dissipative resonance termed R_1. Unlike the Au-Ag materials described above, the optical extinction

spectra shown in Figure 2d and 2e largely comprise of optical absorption rather than scattering. Further, the behaviour of this system is consistent with reported properties of typical Au and Ag particles, and the non-dissipative R_1 resonance is not observed at this stage.

We speculate that this synthesis can potentially lead to five different but related phases. Our speculation is based on available experimental data as well as theoretical advances and is meant to serve as a guide for researchers attempting to replicate this synthesis. Potential outcomes believed possible at the time of this submission are:

1) Ordinary Au and Ag metallic phases
2) Intrinsic/Perfect R_1 Phase
   (Insulator with R_1 resonance, Luminescent when in presence of a near field scatterer, Suppression of optical loss, appears white)
3) Doped/Imperfect R_1 Phase
   (Conductor with R_1 resonance, appears white/gray)
4) Doped/Imperfect R_1 Phase below superconducting T_c
   (Superconductor with R_1 resonance, appears white/gray)
5) Oxidized R_1 Phase
   (Optically lossy conductor with strong paramagnetic/soft ferromagnet-like response, appears black)

In practice, the synthetic outcome will most likely contain a combination of the above phases, depending on experimental skill and precise synthetic conditions. To investigate these above phases, we tried to prepare continuous films out of these nanostructures.

In order to prepare films from the above Au-Ag dispersion, it becomes necessary to precipitate the nanoparticles from solution. We found that centrifugation alone is insufficient to separate the colloids from water. However, partial precipitation could be variously achieved by addition of reagents such as isopropanol (IPA), acetone or acids. Typically, 3 ml IPA was added to ~19 ml of the original solution gradually. This leads to an apparent darkening of the original solution. Optical spectra shown in Figure 2e are broadly consistent with the partial aggregation induced coupling between the original particles. This figure shows the effects of addition of 3 ml of IPA into the solution. The usage of alternatives discussed above leads to qualitatively similar effects. Addition of greater amounts of IPA leads to the formation of larger aggregates that are unsuitable for further processing or measurements.

Following this step, the solution is combined with an equal volume of acetone and the solution was centrifuged (4100 RCF, 4 min). The partially aggregated nanoparticles appear as a dark precipitate on the sides of the centrifuge tube. The supernatant is typically clear and is inferred to be free from residual nanoparticles. This clear liquid is discarded. The solid residue is dried under a rough vacuum (~10 mbar) and is subsequently dispersed in chloroform. Typically, 0.4 ml $CHCl_3$ is used to dissolve the entire products of a reaction. The chloroform dispersions are unstable and must be utilized rather quickly (within ~30 minutes).

We further note that performing the process steps so far under the atmosphere or else in an inert environment does not lead to qualitatively different results. However, all subsequent processing must necessarily be performed under an inert environment (at least <10 ppm of O_2; preferably ~1 ppm O_2). Further, as we show later, the material that results after the procedure described below is extremely oxygen sensitive and is prone to eventual deterioration unless encapsulated.

Films of the Au-Ag material were therefore cast in a nitrogen glove box. Typically, the entire reaction output was dissolved into 0.4 ml of $CHCl_3$. Subsequently, films were drop-cast onto the chrome-gold patterned glass substrate. Each cast corresponds to roughly 5 µl of solution. After drying, the residue is washed with saturated KOH in IPA to remove residual surfactants. Following this, the film was again washed with methanol to remove KOH residues. This process was repeated 50 times, or longer if desired, creating a ~7 mm^2 area film.

Figures 3a-f show the structural characteristics of these materials. In order to collect these data, films were directly cast onto a graphite coated copper grid. A (300 kV) Themis TITAN transmission electron

microscope (TEM) was used to collect all data. Figure 3a shows a low resolution TEM image of the material formed following the steps outlined above. As evident, these processing steps lead to the formation of a polydisperse ensemble of Au-Ag nanostructures. These nanostructures comprise of a polydisperse ensemble of individual particles with an average size of 14 nm. Figure 3b and 3c show aspects of their crystallographic characteristics. In particular, as shown in Figure 3b, the particles show a selected area electron diffraction (SAED) pattern that agrees well with the patterns typically observed in the case of Au and Ag. The most significant planes are marked. We note that forbidden reflections at 0.37 nm are also observed. These are typically seen in the case of twinned or otherwise defective nanoparticles [19-21]. We therefore infer conservation of the lattice parameters of the two metals in these Au-Ag nanostructures. These aspects are also seen in the high resolution TEM (HRTEM) image in Figure 3c. Here, both single crystalline as well as polycrystalline particles are seen to be present within the ensemble. Figure 3d-f show composite high annular aperture-dark field (HAADF) and elemental composition maps of the samples. As evident, the nanoparticles comprise of Ag nanoparticles embedded into an Au matrix. Further, a small number of individual, free Ag particles are also observed.

Figure 4a shows the reflectivity of a typical film cast in this fashion (orange, solid). For comparison, the reflectivity of an ordinary Au nanoparticle film (green, dashed) is also shown. As evident, the Au nanoparticle film shows features characteristic of the localized surface plasmon resonance of gold in the ~2 eV region. It is noteworthy that these features are entirely absent in the case of the Au-Ag nanostructure film prepared through this route. This suggests suppression of Au and Ag plasmons and their replacement by a new resonance R_1 that has been described in reference[7].

Along with this unconventional optical response of Au-Ag materials, we found that air exposure also strongly influences their properties. To illustrate this aspect, we prepared a film of Au-Ag on a quartz substrate. Figure 4b shows the optical transmission spectrum of this film (green curve). To collect this spectrum, the film was covered with another quartz slide and the gap between the two slides was sealed with vacuum grease. Care was taken to prevent contact between the film and the sealant. As evident, an approximately 80% specular transmittance was observed over the entire spectral range, with no clear features in the visible region. This is consistent with the grey-white appearance of the as-prepared film (Figure 4c). Following this measurement, the quartz substrates were separated, and the film was allowed to be exposed to air. The effects of 6 (red) and 30 (brown) minutes of air exposure are further shown in Figure 4b. Clearly, air exposure causes a fall in the film transmittance to ~20%. Visually, this is accompanied by noticeable darkening of the film (Figure 4d; film was moved back into the inert environment after 30 minutes of air exposure and photographs were taken within the inert environment). We found that these changes are permanent in most cases and in general cannot be reversed completely by chemical means.

We observe that the optically lossy air exposed state exhibits finite resistance at all temperatures. Further, it exhibits a magnetic response that may be described as that of a soft ferromagnet. The magnetic character appears to increase with air exposure. This transformation is not associated with any distinct structural transformations. We additionally find that the treatment of the air-exposed material by known reductants (e.g., sodium borohydride or ascorbic acid) does reverse the process partially in some cases and completely in very rare instances where the air exposure is mild. It is known that the material is otherwise stable to nitrogen, water and water soluble carbonates and bicarbonates. Since oxygen is the main remaining constituent of air as well as a paramagnet in its ground state, as well as reactive to reducing agents, we tentatively ascribe this phenomenon to originate from the coverage of the Au-Ag material by a layer of di-oxygen.

In conclusion, we describe the synthetic considerations adopted to prepare Au-Ag nanostructures. The methodology adopted as well as the material structure bear resemblance to semiconductor nanostructure assemblies formed through charge transfer. The preparation involves preparation of Ag nanoparticles and the subsequent formation of Au particles in the growth solution. The key step involves the addition of a destabilizer such as IPA that causes the partial aggregation. Following this process, the aggregates are collected and separated through centrifugation. Films are necessarily cast in an inert environment. We also presented a strong oxygen dependency of these Au-Ag materials which is quite unique and necessities further investigation.

Methods section

Materials used for synthesis:

Hexadecyltrimethylammonium bromide from Sigma(≥98% pure, Lot number SLBT7256)[1], sodium hydroxide from SDFCL(AR grade), ammonium bromide from SDFCL (extrapure) , potassium iodide from Sigma-Aldrich(ACS reagent, ≥99.0% pure), silver nitrate from Sigma-Aldrich(ACS reagent,≥99.0% pure), sodium borohydride powder from Sigma-Aldrich(≥98.0% pure), hydrogentetrachloroaurate(III)trihydrate from Sigma-Aldrich(ACS, 99.99% pure, metal basis), propan-2-ol from SDFCL(AR,ACS grade) and acetone from SDFCL(AR,ACS grade) were used as received

Synthesis of Au/Ag clusters:

Aqueous solutions of 0.1M hexadecyltrimethylammonium bromide (10 mL), 0.1M NaOH (0.1 ml), 1 M ammonium bromide (1 mL), 0.1 M potassium iodide (40 µL) and 1 mM silver nitrate (5 mL) were mixed. The mixture was continuously stirred at 1000 rpm followed by addition of 2 mL of 0.1 M aqueous solution of sodium borohydride after ~90 s to produce the silver nanoparticles.

Then 800 µL of 1mM aqueous solution hydrogentetrachloroaurate (III) trihydrate was added to the silver clusters followed by 3 mL of propan-2-ol. The resulting solution and acetone were mixed in the ratio 1:1 by volume and centrifuged for 3-4 min at 4100 RCF. After centrifugation, the supernatant was discarded, and the precipitate was dried in vacuum. The dry precipitate was dissolved in chloroform to make the film.

Procedure followed for making films:

5 µl of redispersed sample precipitate was drop casted on the required substrate inside the glove box. When chloroform got evaporated, 30 µl of saturated KOH in IPA solution was added to the film and kept for 1 min. After this the excess liquid was discarded and left for drying again. Finally, it was rinsed thoroughly with MeOH and dried well. This process was repeated till a film of desired connectivity is achieved.

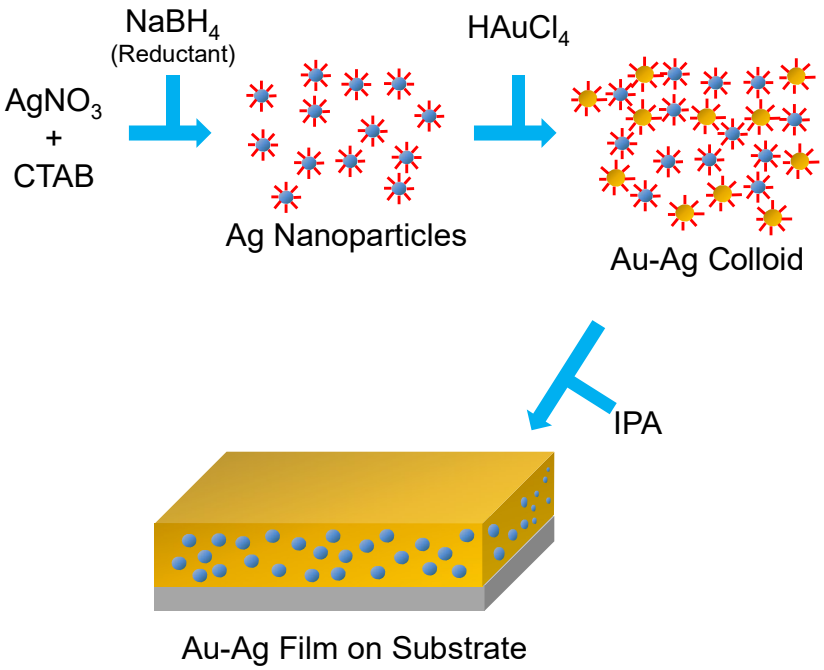

Figure 1. Schematic showing steps for preparation of Au-Ag nanostructures. Prominent reagents are mentioned. Details are described in text.

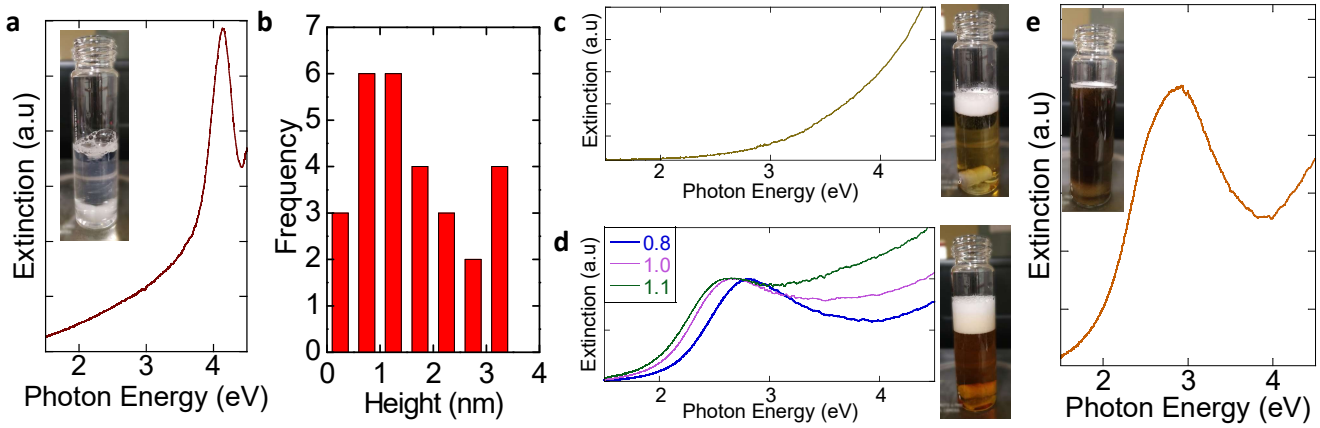

Figure 2. a. Optical extinction spectrum of $AgNO_3$-CTAB dispersion immediately before borohydride addition. Inset: Photograph of an exemplary reaction mixture. **b.** Histogram of sizes of Ag nanoparticles. **c.** Optical extinction spectrum and an exemplary photograph of Ag nanoparticles. **d.** Optical extinction spectra of Au-Ag colloids with varying $HAuCl_4$ addition showing redshift of the Au related extinction feature. The spectra correspond to addition of 0.8 ml (blue), 1.0 ml (violet), 1.1 ml (green) of 1 mM aqueous $HAuCl_4$. The photograph corresponds to addition of 0.8 ml 1 mM aqueous $HAuCl_4$. **e.** Optical extinction spectrum of Au-Ag colloid after IPA addition. Inset: Photograph of the Au-Ag colloid after IPA addition.

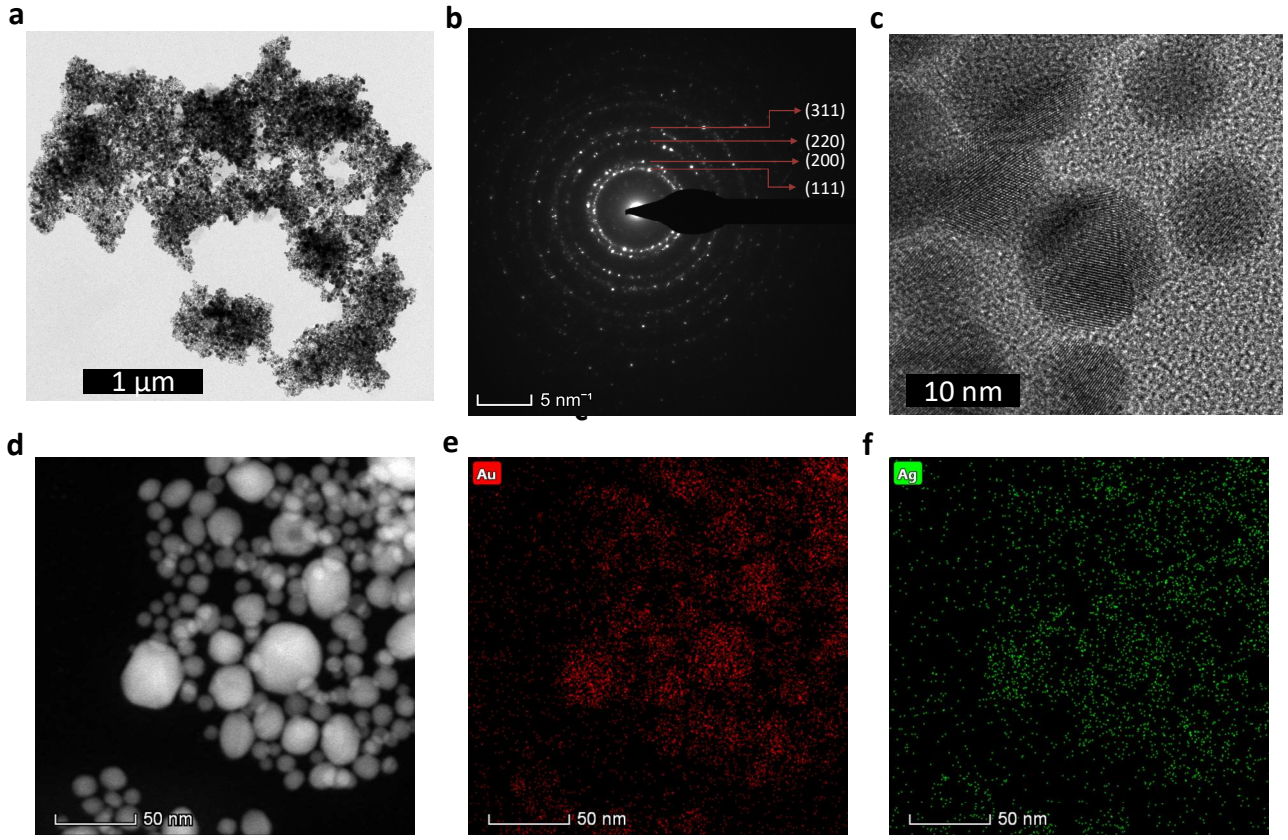

Figure 3. a. TEM of Au-Ag nanostructures. **b.** SAED pattern of Au-Ag nanostructures. Important planes are labelled. **c.** HRTEM of Au-Ag nanostructures **d.** HAADF of Au-Ag nanostructures. **e.** and **f.** are elemental mapping of Au and Ag respectively.

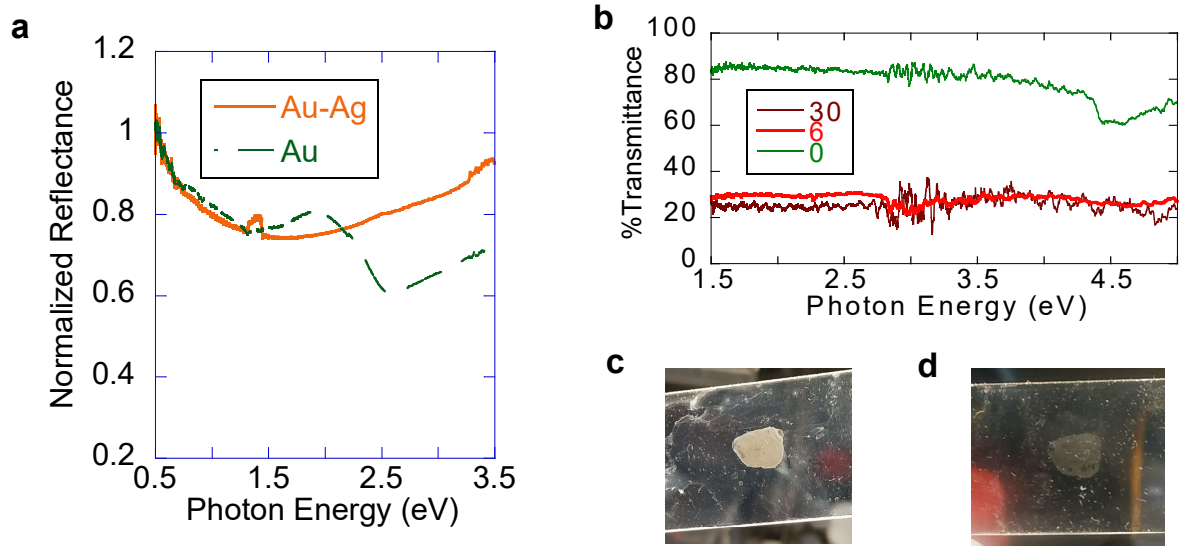

Figure 4 a. Optical Reflectance of Au-Ag nanostructure film (solid) and Au nanoparticle film (dashed) cast on quartz. **b.** Reflectance of an Au-Ag nanostructure film on a quartz substrate measured for the quartz encapsulated film (0, green) and after 6 and 30 minutes of air exposure after the encapsulation was removed. **c.** Photograph of the pristine film **d.** Photograph of the film after 30 minutes of air exposure.

Acknowledgements

AP acknowledges support from the Indian Institute of Science under an IOE scheme. Further, AP acknowledge DST SERB IRHPA [IPA/2020/000033] for additional support. PM thanks MHRD, GoI for a Prime Minister's Research Fellowship. NV thanks DST-Inspire Fellowship.

References

[1] Ashcroft N W and Mermin N D 1976 *Solid State Physics*: Harcourt College Publishers
[2] Thapa D K and Pandey A 2018 Evidence for Superconductivity at Ambient Temperature and Pressure in Nanostructures *arXiv preprint arXiv: 1807.08572v1*
[3] Dalai M K, Singh B B, Sethy S K, Sahoo S P and Bedanta S 2019 Superconductivity in Ag implanted Au thin film *arXiv preprint arXiv:1906.02091*
[4] Hooda M, Kumar P, Balakrishnan V and Yadav C 2019 Observations of zero electrical resistance of Au-Ag thin films near room temperature *arXiv preprint arXiv:1906.00708*
[5] Islam S, Mahadevu R, Saha S K, Mahapatra P S, Bhattacharyya B, Thapa D K, Sai T P, Patil S, Pandey A and Ghosh A 2019 Current-voltage characteristics in Ag/Au nanostructures at resistive transitions *arXiv preprint arXiv:1906.02291*
[6] Mahapatra P S, Saha S K, Mahadevu R, Islam S, Mondal P, Kumbhakar S, Sai T P, Patil S, Chandni U and Pandey A 2019 Observation of excess resistance anomaly at resistive transitions in Ag/Au nanostructures *arXiv preprint arXiv:1912.05428*
[7] Thapa D K, Saha S K, Bhattacharyya B, Rajasekar G P, Mahadevu R and Pandey A 2019 Unconventional Optical Response in Engineered Au-Ag Nanostructures *arXiv preprint arXiv:1906.05342*
[8] Dolgopolov S 2015 Formation of Cooper Pairs as a Consequence of Exchange Interaction *arXiv preprint arXiv:1501.04978*
[9] Baskaran G 2018 Theory of Confined High Tc Superconductivity in Monovalent Metals *arXiv preprint arXiv: 1808.02005*

[10] Mahadevu R and Pandey A 2014 Ionic Bonding between Artificial Atoms *The Journal of Physical Chemistry C* **118** 30101-5
[11] Mahadevu R and Pandey A 2018 Thermodynamic Model for Quantum Dot Assemblies Formed Because of Charge Transfer *ACS Omega* **3** 266-72
[12] Baida H, Billaud P, Marhaba S, Christofilos D, Cottancin E, Crut A, Lermé J, Maioli P, Pellarin M and Broyer M 2009 Quantitative determination of the size dependence of surface plasmon resonance damping in single Ag@ SiO2 nanoparticles *Nano letters* **9** 3463-9
[13] Crut A, Maioli P, Del Fatti N and Vallée F 2014 Optical absorption and scattering spectroscopies of single nano-objects *Chemical Society Reviews* **43** 3921-56
[14] Lermé J, Baida H, Bonnet C, Broyer M, Cottancin E, Crut A, Maioli P, Del Fatti N, Vallée F and Pellarin M 2010 Size Dependence of the Surface Plasmon Resonance Damping in Metal Nanospheres *The Journal of Physical Chemistry Letters* **1** 2922-8
[15] Yu C, Schira R, Brune H, von Issendorff B, Rabilloud F and Harbich W 2018 Optical properties of size selected neutral Ag clusters: electronic shell structures and the surface plasmon resonance *Nanoscale* **10** 20821-7
[16] Gaudry M, Lermé J, Cottancin E, Pellarin M, Vialle J L, Broyer M, Prével B, Treilleux M and Mélinon P 2001 Optical properties of $(Au_xAg_{1-x})_n$ clusters embedded in alumina: Evolution with size and stoichiometry *Physical Review B* **64** 085407
[17] Kreibig U and Vollmer M 2013 *Optical properties of metal clusters* vol 25: Springer Science & Business Media
[18] Genzel L, Martin T and Kreibig U 1975 Dielectric function and plasma resonances of small metal particles *Zeitschrift für Physik B Condensed Matter* **21** 339-46
[19] Lisiecki I 2005 Size, Shape, and Structural Control of Metallic Nanocrystals *The Journal of Physical Chemistry B* **109** 12231-44
[20] Lisiecki I and Pileni M P 1995 Copper Metallic Particles Synthesized "in Situ" in Reverse Micelles: Influence of Various Parameters on the Size of the Particles *The Journal of Physical Chemistry* **99** 5077-82
[21] Liu M and Guyot-Sionnest P 2005 Mechanism of Silver(I)-Assisted Growth of Gold Nanorods and Bipyramids *The Journal of Physical Chemistry B* **109** 22192-200